DOR: 20.1001.1.27170314.2023.12.1.3.6

Research Paper

Investigation of Effective Plastic Strain Heterogeneity and the Effect of Using Interface Sheet in Constrained Groove Pressing of Copper Sheet

Moein Gholami[1], Ali Hasanabadi[2*]
[1]PhD Candidate, Mechanical Engineering Department, University of Birjand, Birjand, Iran
[2]Assistant Professor, Mechanical Engineering Department, University of Birjand, Birjand, Iran
[*]Email of Corresponding Author: hasanabadi@birjand.ac.ir
Received: January 9, 2023; Accepted: March 2, 2023

Abstract

The constrained groove pressing process is one of the most effective methods of severe plastic deformation to produce very fine-grained sheet metal. Numerical simulation is performed in several steps by finite element software in such a way that the output result of each step, which is strain-hardened, is used as the input of the next step. The finite element results of the obtained plastic effective strain distribution show that the strain changes along the longitudinal direction of the sample are oscillating. The relevant results also show that in the direction of thickness, the amount of strain in the middle of the sample is maximum and as it moves away from the center of the sample, the amount of strain decreases. In addition, the results of strain heterogeneity show that the strain heterogeneity factor in the longitudinal direction is 2.8 times the corresponding value in the thickness direction whereas the average plastic strain in the two directions differs only about 13.4%. Then, to improve the strain uniformity, steel sheets are placed at the top and bottom of the sample as interface sheets, and then the constrained groove pressing is applied. Using this method, it is observed that the degree of strain homogeneity in the first stage is improved compared to the conventional method of the constrained groove pressing process. By using this method, it can be seen that the amount of strain heterogeneity factor is reduced from 6.85 to 2 in the first stage.

Keywords

Severe Plastic Deformation, Constricted Groove Pressing, Copper Sheet, Numerical Analysis, Strain Distribution Heterogeneity

Symbols and Abbreviations

γ_{xy}	Engineering shear stress	Cx	Strain heterogeneity coefficient
H	Groove height	S	The standard deviation of plastic strain
T	Groove width	θ	the angle of the mold groove
ε_{xy}	True shear strain	ne	number of nodes
ε_{eff}	effective strain	n	strain-hardening exponent
$\bar{\varepsilon}$	average effective strain	K	strength coefficient
ε_i	effective strain in the i-th node	CGP	Constrained Groove Pressing
ε_{total}	Total effective plastic strain	ISCGP	Interface Sheet Constrained Groove Pressing

1. Introduction

Severe plastic deformation methods are processes that change the grain size of the microstructure of materials from micro to nanometer dimensions, leading to the production of products with much higher strength [1, 2]. The common feature of the processes of severe plastic deformation in sheets is the stability of the dimensions and the non-change of the appearance of the sheet during the process, as a result of which the limitation of the application of strain disappears. Metals that undergo severe plastic deformation processes have very good properties such as high strength at ambient temperature, wear resistance, superplastic property at high temperature and low strain rate, good fatigue properties, and excellent corrosion resistance [3, 4]. Severe plastic deformation processes include several methods such as constrained groove pressing (CGP) [5, 6], Equal channel angular pressing [7, 8], high-pressure torsion [9, 10], and accumulative roll bonding [11, 12]. Most of these methods require expensive tools and complex procedures [13, 14]. The CGP process was first developed in 2002 by Shin et al. [15]. They applied this process on aluminum sheets and concluded that with this method, fine graining and thus improving the mechanical properties of metal sheets is possible.

Sajadi et al. [16] studied the forming force in the CGP process of the aluminum sheet using the finite element method. They simulated the CGP process in three different conditions: 2D and plane stress, 2D and plane strain, and 3D, and compared these three methods with each other as well as experimental tests. Their results showed that two-dimensional simulation with plane strain conditions matches well with three-dimensional conditions and experimental tests.

Honarpisheh et al. [17] experimentally and numerically investigated the CGP process on pure copper samples with a thickness of 3 mm and concluded that it is possible to improve the mechanical properties by performing the constrained groove pressing process. They also showed that the strain changes in the longitudinal direction are fluctuating. Finally, they presented a relationship that can estimate the yield stress based on Vickers hardness with high accuracy. In another research [18], these researchers investigated the effect of the CGP process on the residual stress distribution of copper samples experimentally and numerically and concluded that the residual stress distribution on the surface of the sample is compressive and as it approaches the central layers, these stresses are converted into tension residual stress. In addition, the distribution of residual stress in the direction of length and thickness is reported to be almost uniform.

Nazari et al. [19] investigated the effect of the friction coefficient in the CGP process on the residual stresses and reported that the friction coefficient has a direct relationship with the residual stress.

Niranjan et al. [20] investigated the effect of the aluminum sheet bound groove pressing process on the deep drawing process and showed that performing the above process on these sheets improves the ability of the deep drawing process. Hosseini et al. [21] predicted the stress-strain curve by using a material behavior model that is based on physical and metallurgical assumptions assuming the state of dislocation density to be variable.

Wang et al. [22] theoretically and experimentally investigated the effect of die angle and groove width on the mechanical and microstructural properties of nickel sheets under the CGP process and reported that increasing the width and angle of the grooves increases the force of the process. In another research [23], these researchers investigated the effect of friction experimentally in the process of bound groove pressing and showed that by improving the surface conditions, it is possible to apply a higher number of passes.

One of the important characteristics of mechanical properties is the uniformity of material properties. Due to the nature of the process, there is a non-uniform distribution of strain and, as a result, non-uniformity of the structure in the CGP process. Yadav et al. [24] investigated the effect of the restricted groove pressing process on the non-uniformity of the microstructure and concluded that the CGP samples have local non-uniformity that repeats sinusoidally in the material structure.

According to the background of the reviewed research, it has been reported that the strain distribution and consequently the mechanical properties are non-uniform in the CGP process.

One of the weaknesses of the CGP process is the non-uniform strain distribution that causes the non-uniform distribution of mechanical properties in the material structure due to the relationships between applied strain and mechanical properties. This effect can limit the use of deformed samples for some applications.

In this research, to increase the uniformity of the strain distribution, the possibility of using an interface sheet has been investigated, which can improve the uniformity of applied plastic strain. It should be mentioned that the uniformity of the mechanical structure is related to the uniformity of applied strain. In other words, the greater the uniformity of the plastic strain in the deformed sample, the greater the isotropic of the deformed sample.

2. Constrained groove pressing process

In the CGP process, a full pass consists of four consecutive steps, two steps are performed by groove dies, and two steps by flat dies. In the first step of each pass, a metal sheet of thickness t is placed between two grooved dies with width T, height H, and groove angle θ according to Figure1(a). If the value of the angle θ is equal to 45°, the value of H and T will be equal. The lower die is fully restrained and the upper die can move vertically. After the dies are close to each other, the parts of the sheet that are in the inclined areas of the dies are subjected to deformation by shear stress according to Figure 1(a), whereas the flat areas of the sheet are not deformed. In the second step of each pass, as shown in Figure 1(b), the metal sheet is compressed by a pair of simple flat dies, which causes the areas of the sheet that were deformed in the first step to undergo a reverse shear deformation, and the sheet becomes flat. After the end of the second step and before the implementation of the third and fourth steps of the process, the workpiece is rotated 180 degrees around its thickness axis so that the deformed areas in the first step are on the flat areas of the grooved die and the flat areas that are not deformed previously are on the inclined areas of the die.

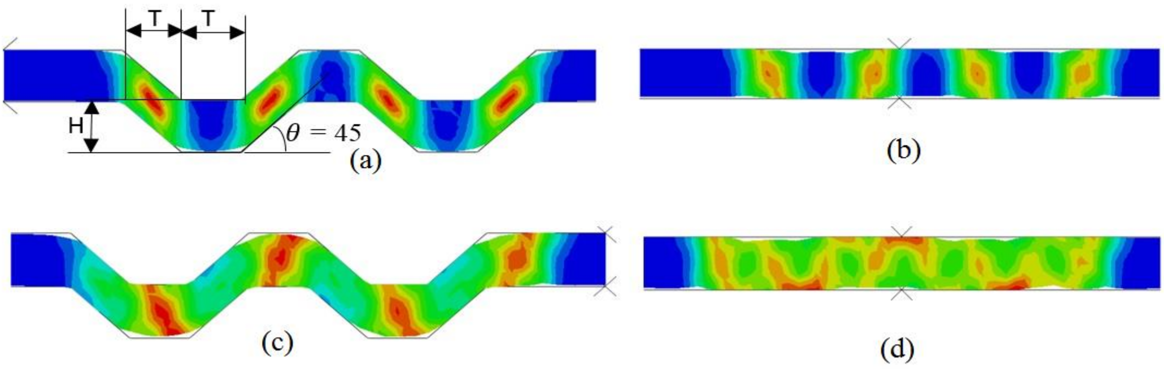

Figure 1. Schematic of the CGP process steps

In the finite element simulation in two-dimensional conditions, due to the impossibility of rotating the workpiece, a die with a similar shape to the mold of the first stage has been created to satisfy the condition of rotating the sample. In finite element simulation in two-dimensional conditions, due to the impossibility of rotating the workpiece, the die geometry is changed in a way to create the real die conditions as demonstrated in Figures 1(c) and 1(d).

3. Ideal effective shear strain

To compare the finite element simulation results, the effective shear strain value can be obtained ideally based on the die geometry as depicted in Figure 2. According to Figure 2, the amount of effective strain after the first step of the CGP process is calculated in the deformed areas of the sheet. Engineering shear strain can be obtained from Eq. (1):

$$\gamma_{xy} = \frac{H}{T} = \tan\theta \qquad (1)$$

The value of shear strain ε_{xy} is half of the value calculated in Eq. (1).

$$\varepsilon_{xy} = \frac{\gamma_{xy}}{2} \qquad (2)$$

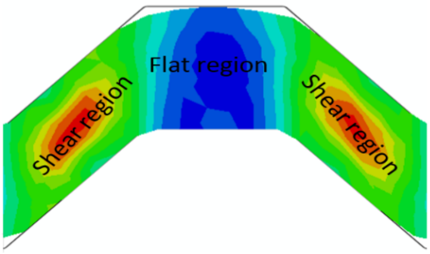

Figure 2. Schematic representation of a part of the sheet after deformation in the first step of the CGP process

Assuming pure shear deformation under plane strain conditions ($\varepsilon_x = \varepsilon_y = \varepsilon_z = \varepsilon_{yz} = \varepsilon_{zx} = 0$), the effective strain created in the deformed areas after each step in the CGP process is calculated from Eq. (3) [20]:

$$\varepsilon_{total} = n\,\frac{2tan\theta}{\sqrt{3}} \qquad (3)$$

If the angle of the mold groove, θ is equal to 45 degrees, the width of the groove, T, will be equal to the height of the groove, H, and as a result, the engineering shear strain is equal to $\gamma_{xy} = 1$, and in each step, the effective strain is equal to $\varepsilon_{eff} = {}^{1}/_{\sqrt{3}} \approx 0.58$ will be applied to the deformed areas. Therefore, from a theoretical point of view, one cycle of the CGP process with this groove angle, if the total stress is considered as shear stress, leads to the application of a total effective strain equal to 1.16 on the sheet [22].

4. Finite element simulation

In this research, finite element simulation of the CGP process in two different models is done by ABAQUS software on a copper sheet in plane strain conditions. The first model of a 2 mm thick copper sheet is subjected to a full pass of the CGP process. In the second model, the copper sheet is placed between two 304 stainless steel sheets as interface sheets, and only the first stage of the CGP process will be simulated, and by comparing the amount of the effective plastic strain distribution, the effect of the interface sheets will be considered in the CGP process. The mechanical properties of the annealed copper and steel sheets used in the simulation are presented in Table 1.

Table 1. Mechanical properties of the materials [25]

Material	K(MPa)	n
Copper	530	0.44
304 stainless steel	1400	0.44

Finite element simulation has been done assuming plane strain conditions and with dimensions of die and workpiece equal to 2 × 20 mm and dies groove angle of 45 degrees.

In this simulation, the value of the friction coefficient according to Ref. [23] is considered as 0.25. At each step of the analysis, the degrees of freedom of the bottom die (flat and grooved) are constrained in all directions. The upper part of the die can only be moved perpendicularly to the sheet. The amount of displacement of the die during the deformation process is the amount of sheet thickness and the sides of the sheet are also constrained. In this simulation, according to the shape of the sheet, the two-dimensional element CPE4R is used for meshing the sheet. This is a square element with one degree of freedom for each node, which prevents shear locking by using reduced integration. Figure 3 shows the sensitivity diagram of the element size for the amount of plastic strain in the simulation of the first stage of the process. According to Figure 3, with the reduction of the element size from 0.35 mm, the strain variable does not change significantly. Therefore, in the finite element model, 348 elements with a size of 0.35 have been used to analyze the sheet.

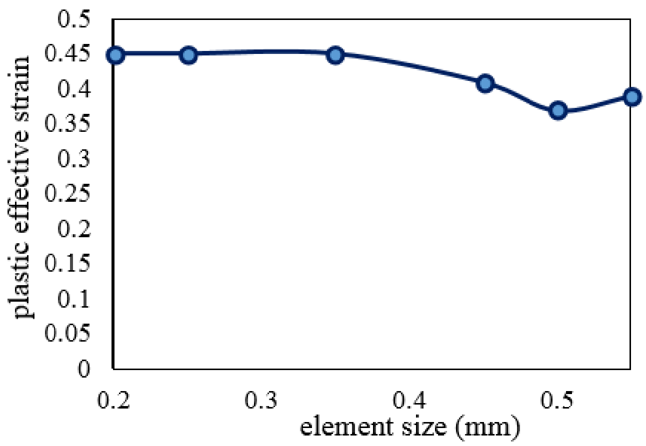

Figure 3. Diagram of sensitivity to element size in terms of effective plastic strain

Figure 4 shows the grooved dies and flat dies in finite element simulation.

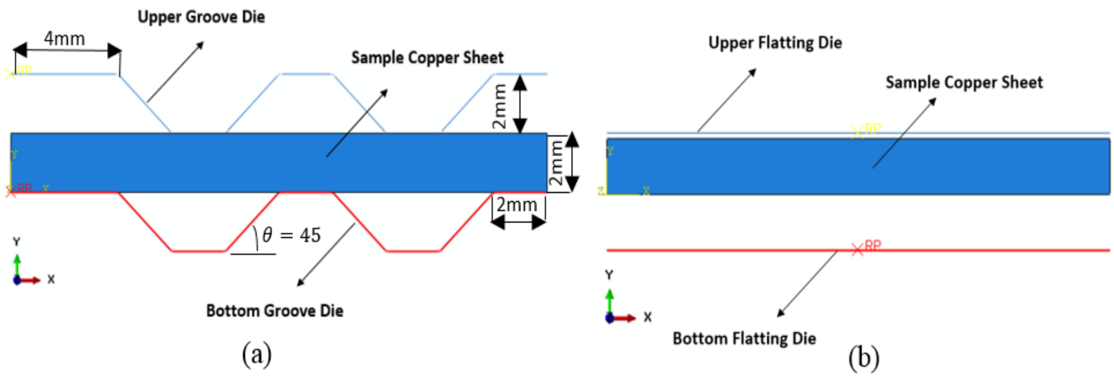

Figure 4. (a) Grooved dies, (b) flat dies in finite element simulation

5. Results and discussion

5.1 Accumulated plastic strain distribution

Figure 5 shows the simulation results for a complete cycle of the constrained groove pressing process. These results include effective plastic strain contours in four steps. As it is known, the accumulated effective plastic strain increases during four steps. Also, the results show that the areas that have not deformed in the first two stages have the highest amount of strain in the sheet in the third and fourth steps.

According to Figure 5, in the first step, the inclined regions have undergone deformation, while the flat regions have remained unchanged. In the second step, from the first pass, the deformed areas in the first step are subjected to reverse shear deformation, and the amount of effective plastic strain increases by about two times, while the unreformed areas remain unchanged. In the third and fourth steps (rotation of the sheet 180 degrees around the thickness axis), the areas that have not deformed in the first and second steps undergo deformation according to the stated process.

Ideally, it is expected that after the end of the fourth step (the completion of the first pass), the strain distribution in the sheet is uniform, but according to Figure 5, the distribution of the effective plastic strain at the end of the fourth stage is non-uniform. To better investigate the distribution of the effective plastic strain in the four steps of the CGP process, a path in the middle of the sample, located on the nodes of the center line (line 1 in Figure 5) was defined at equal intervals. Figure 6 shows the effective plastic strain distribution diagrams for the four steps on this line.

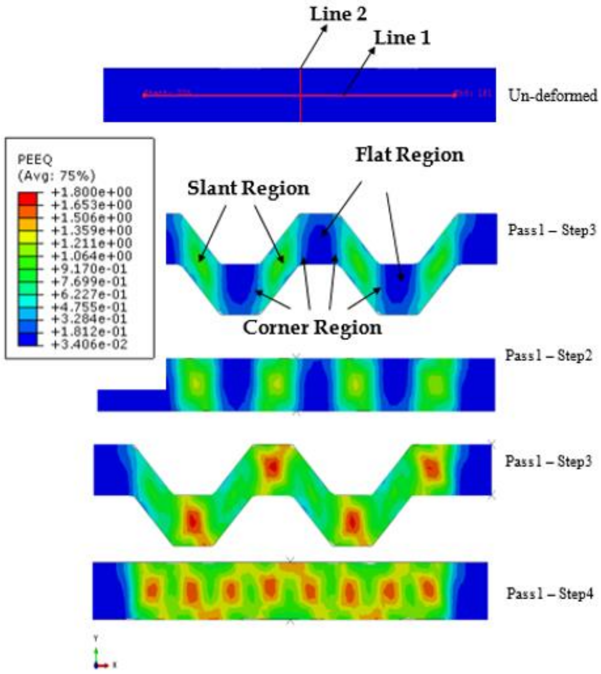

Figure 5. Effective plastic strain contours in four steps

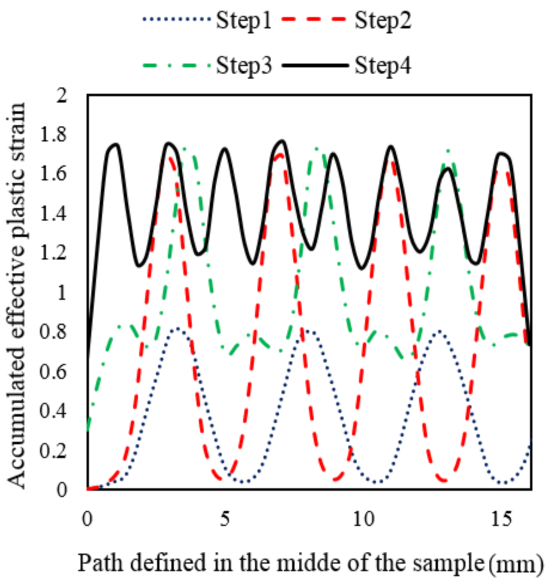

Figure 6. Plastic effective strain distribution diagrams for the four steps of the CGP process (Line 1 in Figure 5)

According to Figure 6, in the first step of the first pass, the amount of effective plastic strain changes from the lowest value in the flat areas (strain value equal to 0.016) to the highest value in the inclined areas of the grooves (strain value equal to 0.87). In the second step, the maximum effective plastic strain in groove areas has reached 1.60, while the strain in flat areas has remained at minimum values. According to this trend, the average accumulated plastic strain in the third and fourth steps reaches about 0.99 and 1.27, respectively. Ideally, based on the analytical model, the plastic strain values at the end of the first and second steps should reach 0.58 and 1.16, respectively, but according to Figure 6, it can be seen that the results obtained from finite element simulation are more than these values.

The reason is that in the CGP process, due to the geometry of the die, in addition to the shear strain, other deformations also occur. This case has been observed both in simulation and in practice [26]. In Table 2, the average effective plastic strain obtained from finite element simulation at the end of the fourth step is compared with other research. Due to the different conditions created during the process, the amount of plastic strain accumulation in different areas of the sheet is not the same and fluctuates between 0.63 and 1.66. One of the reasons for this non-uniformity can be attributed to the edge radius of the die groove [27]. The presence of the corner radius makes the areas of the sheet in contact with it, to be exposed to less shear deformation than the inclined and flat areas.

Table 2. Comparison of average effective plastic with other research

Researchers	Material	Average effective plastic strain
Sunil Kumar et al [27]	AA5083	1.22
Siddesha et al [26]	Pure aluminum	1.66
M. Honarpisheh et al [17]	Pure Copper	1.31
Current study	Copper	1.27

The distribution of plastic strain in the thickness direction (line 2 in Figure 5) is shown in Figure 7. It can be seen that the accumulation of effective plastic strain is maximum in the center of the sheet in the direction of thickness and has a decreasing trend from the center towards the surface of the sample. This means that in the CGP process, less strain is created on the surface of the sample. These results agree with the results reported in related research [15-17].

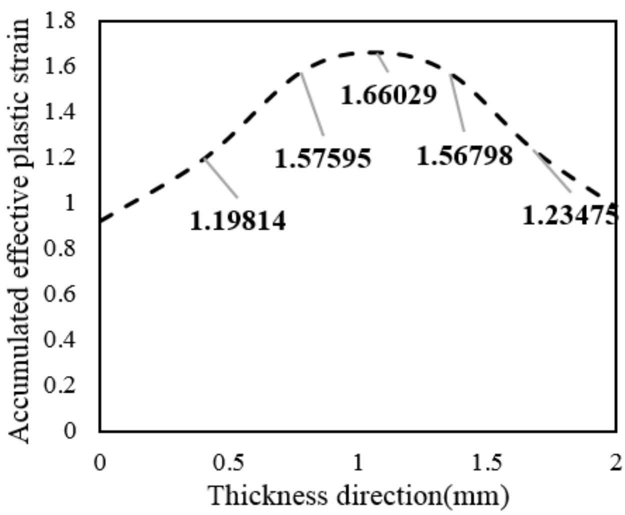

Figure 7. Effective plastic strain distribution on line 2 of Figure 5 (in the direction of thickness)

The average effective plastic strain in the direction of thickness is 1.44 which is more than the similar case in the longitudinal direction. This is consistent with the results reported in Ref. [17].
The results of the simulation confirm the non-uniformity of the strain in the CGP method, which has also been mentioned in previous research [17, 28]. Non-uniform strain distribution causes non-uniformity in mechanical properties such as hardness [29], which can be undesirable.

5.2 Accumulated plastic strain heterogeneity

Due to the existence of friction as well as the geometry of the die, the existence of heterogeneity in the output of the CGP process is inevitable. From Eq. (4), the amount of strain heterogeneity can be calculated [30]:

$$Cx = \frac{S}{\bar{\varepsilon}} \qquad (4)$$

whereas Cx is the heterogeneity factor, $\bar{\varepsilon}$ is the average effective strain, and S is the standard deviation of the effective strain, which is calculated using Eq. (5) [30].

$$S = \sqrt{\frac{\sum_{i=1}^{ne}(\varepsilon_i - \bar{\varepsilon})^2}{ne-1}} \qquad (5)$$

whereas, ε_i is the effective strain in the i-th node and ne is the number of nodes. Figure 8 shows the strain heterogeneity coefficient diagram for the four stages of the first pass of the CGP process. According to Figure 8, it can be concluded that the amount of heterogeneity in different steps of the CGP process is almost the same, which can be justified considering the nature of the process and the similarity of its operation in different steps. Figure 9 shows the changes in the heterogeneity coefficient after the first pass of the CGP process for both length and thickness directions. It can be seen that the amount of strain heterogeneity in the thickness direction is lower than in the longitudinal direction.

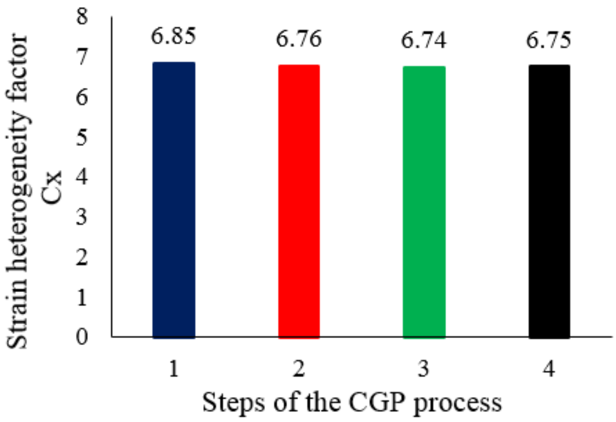

Figure 8. Comparison of the heterogeneity coefficient of the four steps of the first pass of the CGP process

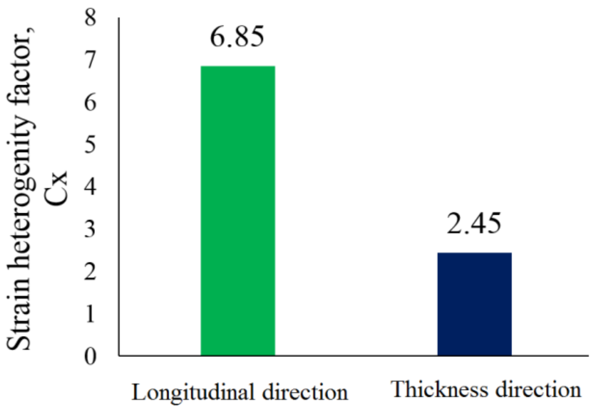

Figure 9. Changes in strain heterogeneity coefficient along the length and thickness of the sample after completion of the CGP process

5.3 Effect of using sheet interface on the level of strain homogeneity

One of the limitations of the CGP process is the non-uniformity of the strain at different points of the sample, which leads to the non-uniformity of the mechanical properties. In this regard, the CGP process is investigated along with the interface sheet [31] at the top and bottom of the sample (Figure 10). As seen in Figure 11, the effective plastic strain distribution diagrams for both CGP and interface sheet-constrained groove pressing (ISCGP) for the first step of the first pass are presented, which show that by using the sheet interface, the maximum strain value is reduced, but the strain distribution becomes more uniform.

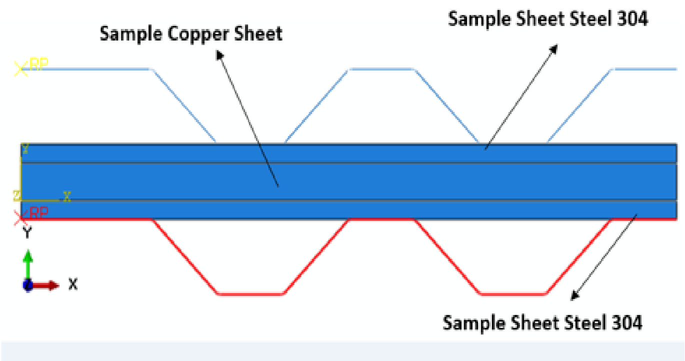

Figure 10. Using 304 stainless steel sheet as interface along with the copper sheet

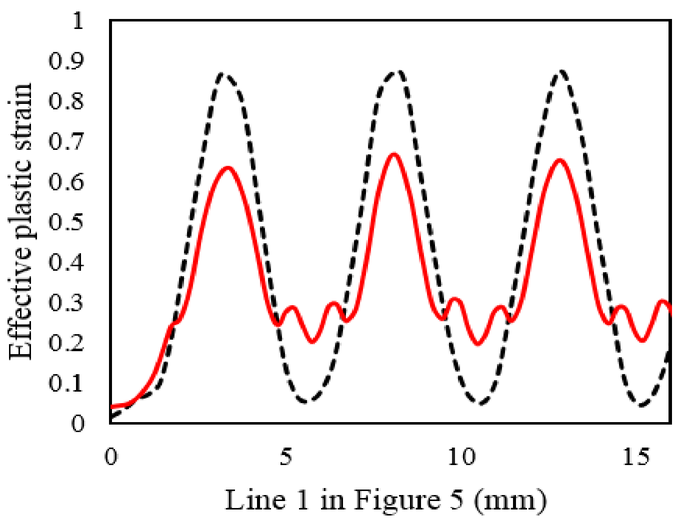

Figure 11. Effective plastic strain distribution diagram for CGP (dashed curve) and ISCGP (red curve) methods

The amount of strain heterogeneity factor by using Eq. (4) and Eq. (5) shows that using the interface sheet (ISCGP) method, the value of the strain heterogeneity factor is reduced from 6.85 to 2. Therefore, the heterogeneity factor in the ISCGP method will be three-tenths of the coefficient of heterogeneity in the CGP method. Decreasing the value of the strain heterogeneity factor means increasing the uniformity of the properties resulting from fineness in different points of the sample. It is reported in the paper [31] that more passes can be applied by using an interface sheet, but the amount of increase in mechanical properties in each pass is slightly lower. In other words, the yield strength obtained by this method is lower than the yield strength of the conventional method, and this issue is related to the accumulation of effective plastic strain created in the sample (Figure 11).

6. Conclusions

In this research, the effects of the CGP process on the heterogeneous distribution of the accumulated strain in the copper sheet and the effective role of the interface sheet in the uniformity of the created strains were studied.

- Although the analytical relations governing the process predict the plastic strain for a complete pass of 1.16, in the simulation it was observed that the average strain in the middle of the sample after the end of the first pass is equal to 1.27.
- Along the length of the sample, the strain changes are fluctuating and the lowest amount of strain occurs in the corner radius regions. The results of strain heterogeneity along the length showed that the amount of strain heterogeneity in different steps of the process does not differ much whereas the maximum strain heterogeneity factor is 6.85 along the length.
- By examining the strain distribution along the thickness of the sample, it was observed that the maximum strain occurs in the center of the sample and as it approaches the surface areas, the amount of strain decreases and in addition, the amount of homogeneity of the strain in the thickness direction is greater than in the longitudinal direction. The amount of average effective strain in the thickness direction is 1.44 which is 13.4% more than the same value along the length direction.
- Even though the use of an interface sheet reduces the maximum amount of applied strain, it has a positive effect on the uniformity of the strain, so the heterogeneity factor, in this case, will be 0.3 of the heterogeneity factor of the CGP process.

7. References

[1] Borhani, M. and Djavanroodi, F. 2012. Rubber pad-constrained groove pressing process: Experimental and finite element investigation. Materials Science and Engineering: A. 546(1):1-7.

[2] Sajadi, A., Ebrahimi, M. and Djavanroodi, F. 2012. Experimental and numerical investigation of Al properties fabricated by CGP process. Materials Science and Engineering: A. 552(1): 97-103.

[3] Peng, K., Su, L., Shaw, L.L. and Qian, K.W. 2007. Grain refinement and crack prevention in constrained groove pressing of two-phase Cu–Zn alloys. Scripta Materialia. 56(11): 987-990.

[4] Peng, K., Zhang, Y., Shaw, L.L. and Qian, K.W. 2009. Microstructure dependence of a Cu–38Zn alloy on processing conditions of constrained groove pressing. Acta Materialia, 57(18): 5543-5553.

[5] Nazari, F. and Honarpisheh, M. 2018. Analytical model to estimate force of constrained groove pressing process. Journal of Manufacturing Processes. 32: 11-19.

[6] Shirdel, A., Khajeh, A. and Moshksar, M. 2010. Experimental and finite element investigation of semi-constrained groove pressing process. Materials & Design. 31(2): 946-950.

[7] Ranaei, M.A., Afsari, A., Ahmadi. Brooghani, S. Y. and Moshksar, M. M. 2014. Microstructure, mechanical and electrical properties of commercially pure copper deformed severely by equal channel angular pressing. Modares Mechanical Engineering.14(15): 257-267.

[8] Nili Ahmadabadi, M., Shirazi, H., Ghasemi-Nanesa, H., Hossein Nedjad, S., Poorganji, B. and Furuhara, T. 2011. Role of severe plastic deformation on the formation of nanograins and nano-sized precipitates in Fe–Ni–Mn steel. Materials and Design. 32: 3526–31.

[9] Ivanisenko, Y.U., Valiev, R.Z. and Fecht, H.J. 2005. Grain boundary statistics in nanostructured iron produced by high pressure torsion. Materials Science and Engneering. 390:159–65.

[10] Horita, Z., Smith, D.J., Furukawa, M., Nemoto, M., Valiev, R.Z. and Langdon, T.G. 1996. An investigation of grain boundaries in submicrometergrained Al-Mg solid solution alloys using high-resolution electron microscopy. Journal of Materials Research. 11(8):1880-1890.

[11] Saito, Y., Tsuji, N., Utsunomiya, H., Sakai, T. and Hong, R. G. 1998. Ultrafine grained bulk aluminum produced by accumulative roll bonding (ARB) process. Scripta Materialia. 39(9):1221-1227.

[12] Saito, Y., Tsuji, N., Utsunomiya, H. and Sakai, H. 1999. Novel ultra-high straining process for bulk materials—development of the accumulative roll-bonding (ARB) process. Acta Materilia. 47: 579–583.

[13] Faraji, G. and Kim, H.S. 2017. Review of principles and methods of severe plastic deformation for producing ultrafine-grained tubes. Materials Science and Technology. 33(8): 905-923.

[14] Torabzadeh, H. and Faraji, G. 2016. A review of the production of ultrafine grained and nanograined metals by applying severe plastic deformation. Modares Mechanical Engineering. 16(6): 271-282.

[15] Shin, D.H., Park, J.J., Kim, Y.S. and Park, K.T. 2002. Constrained groove pressing and its application to grain refinement of aluminum. Material Science and Engineering: A. 328(1-2): 98–103.

[16] Sajadi, A., Ebrahimi, M. and Djavanroodi, F. 2012. Experimental and numerical investigation of Al properties fabricated by CGP process. Materials Science and Engineering: A. 552: 97-103.

[17] Honarpisheh, M., Tavajjohi, M.H. and Nazari, F. 2019. Experimental and Numerical Study of Severe Plastic Deformation in the Constrained Groove Pressing Process on the Pure Copper Sheets. Modares Mechanical Engineering. 19(2): 269-280.

[18] Tavajjohi, M.H. and Honarpisheh, M. 2021. Experimental and numerical study of the longitudinal and transverse residual stresses distribution in the constrained groove pressing process of pure copper sheets. Proceedings of the Institution of Mechanical Engineers, Part L: Journal of Materials: Design and Applications. 236(1): 97-109.

[19] Nazari, F., Honarpisheh, M. and Zhao, H. 2021. Effect of the uncertainty of multi-cut contour method and friction coefficient on residual stresses of constrained groove pressing process. Proceedings of the Institution of Mechanical Engineers, Part C: Journal of Mechanical Engineering Science. 235(11):2039-2052

[20] Niranjan, G. G. and Chakkingal, U. 2010. Deep drawability of commercial purity aluminum sheets processed by groove pressing, Journal of Materials Processing Technology. 210(11): 1511-1516.

[21] Hosseini, E. and Kazeminezhad, M. 2010. Integration of physically based models into FE analysis: Homogeneity of copper sheets under large plastic deformations. Computational Materials Science. 48(1): 166-173.

[22] Wang, Z.S., Guan, Y. and Zhong, C. 2015. Influences of die structure on constrained groove pressing of commercially pure Ni sheets. Journal of Materials Processing Technology. 215: 205-218.

[23] Wang, Z.S., Guan, Y.J. and Zhong, C.K. 2014. Effects of Friction on Constrained Groove Pressing of Pure Al Sheets. Advanced Materials Research. 926: 81-84.

[24] Yadav, P.C., Sinhal, A., Sahu, S., Roy, A. and Shekhar, S. 2016. Microstructural inhomogeneity in constrained groove pressed Cu-Zn alloy sheet. Journal of Materials Engineering and Performance. 25(7): 2604-2614.

[25] Callister, W.D. and Rethwisch, D.G. 2014. Materials Science and Engineering. 9th Edition. Wiley.

[26] Siddesha1, H.S., Shantharaja, M., DilipKumar, K. and Umesh, C.K. 2015. Experimental and computational simulation of production ultra-fine grain structure processed by CGP. International Journal of Advance Research In Science And Engineering. 14(2): 580-591.

[27] Kumara, S., Hariharanb, K., Digavallia, R. K. and Paulc, S. K. 2019. Accounting Bauschinger effect in the numerical simulation of constrained groove pressing process. Journal of Manufacturing Processes. 38: 49–62.

[28] Eftekhari Shahri, S.E., Gholami, M. and Rakhshkhorshid, M. 2022. Numerical-experimental study of die geometry in the constrained groove pressing of 6061 aluminum sheets. doi:10.1177/09544054221138161.

[29] Singh, R., Agrahari, S., Yadav, S.D. and Kumar, A. 2021. Microstructural evolution and mechanical properties of 316 austenitic stainless steel by CGP. Materials Science and Engineering: A. 812: 141105.

[30] Wang, Z.S., Guan, Y.J. and Liang, P. 2014. Deformation efficiency, homogeneity, and electrical resistivity of pure copper processed by constrained groove pressing. Rare Metals. 33: 287–292.

[31] Shahmirzaloo, A., Faraji, G. and Safari, M., Mohammadinejad, S. 2018. Interface sheet-constrained groove pressing as a modified severe plastic deformation process. Materials Science and Technology. 34(14): 1669-1678.